Inorganic Chemistry

Article

pubs.acs.org/IC

The Organozinc Rich Compounds [Cp*M(ZnR)$_5$] (M = Fe, Ru; R = Cp*, Me, Cl, Br)

Mariusz Molon,[†] Christian Gemel,[†] Rüdiger W. Seidel,[‡] Paul Jerabek,[§] Gernot Frenking,*[,§] and Roland A. Fischer*[,†]

[†]Department of Inorganic Chemistry II-Organometallics & Materials and [‡]Department of Analytical Chemistry, Ruhr University Bochum, 44780 Bochum, Germany

[§]Department of Chemistry, Philipps-University Marburg, 35032 Marburg, Germany

Supporting Information

ABSTRACT: Organozinc (ZnR with R = Cp*, Me, Cl, Br) ligated transition metal (M) half-sandwich compounds of general formula [Cp*M(ZnR)$_5$] (M = Fe, Ru) are presented in this work. The new compounds were obtained by treatment of various GaCp* ligated precursors with suitable amounts of $ZnMe_2$ to exchange Ga against Zn. This exchange follows a strict Ga:Zn ratio of 1:2. Accordingly, a Ga/Zn mixed compound [{Cp*Ru(GaCp*)(ZnCp*)(ZnCl)$_2$}$_2$] can be obtained if the amount of $ZnMe_2$ is reduced so that one GaCp* remains coordinated to the transition metal. All new compounds were characterized by elemental analysis, ^{1}H and ^{13}C NMR spectroscopy as well as by single crystal X-ray diffraction techniques, if applicable. The coordination polyhedra of [Cp*M(ZnR)$_5$] can be derived from the pseudo homoleptic parent compound [Ru(ZnCp*)$_4$(ZnMe)$_6$], as emphasized by continuous shape measures analysis (CShM). Computational investigations at the density functional theory (DFT) level of theory were performed, revealing no significant attractive interaction of the zinc atoms and therefore these compounds are best described as classical complexes, rather than cluster compounds. The Ru-L bond strength follow the order Cp* > ZnCl > ZnMe > ZnCp*.

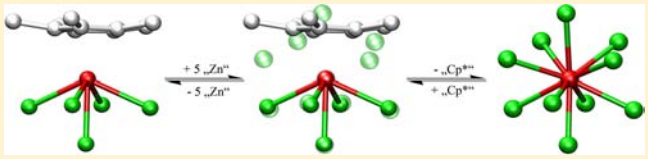

INTRODUCTION

Recently, a new class of homoleptic organozinc ligated complexes of formula [M(ZnR)$_n$] (M = Mo, Ru, Rh, Ni, Pd, Pt; R = Cp*, Et, Me) with unusually high coordination numbers $n \geq 8$ was discovered.[1] These compounds are formed upon treatment of the all-Ga coordinated complexes [M(GaCp*)$_{n/2}$] (M = Mo, Ru, Rh, Ni, Pd, Pt)[2] with excess of $ZnMe_2$ or $ZnEt_2$. The unique reaction involves a correlated and selective Ga/Zn metal and Cp*/Me ligand exchange. Analyses at the density functional theory (DFT) level of theory revealed a bonding situation in between coordination compounds and clusters with weak attractive (at least not repulsive) Zn−Zn interactions. The bonding situation, the validity of the 18 electron rule in all cases, and the rationalization of the structural features of the particular coordination polyhedra of the homoleptic examples have been discussed in detail. For example, while [Mo(ZnR)$_{12}$] is an almost perfect icosahedron, the 10-fold and 9-fold coordinated complexes are best described as centaur polyhedra or singly capped square antiprisms.[3] Both coordination environments are very common in the solid state structures of zinc-rich Hume−Rothery type M/Zn alloys, that is, the compounds [M(ZnR)$_n$] represent "cut-outs" of intermetallic phase structures, wrapped into an organic (all-hydrocarbon) shell.

Two further examples point to a generalization of this exchange concept of two Zn atoms for one Ga atom, which is the basis of a rational synthesis to achieve highly coordinated and zinc-rich products, whose structures can be related to intermetallic solid state compounds. The treatment of the heteroleptic compounds [(CO)$_4$Mo(GaCp*)$_2$][2b] and [Cp*Rh(GaCp*)$_2$(GaCl$_2$Cp*)][4] with excess $ZnMe_2$ lead to comparably complex molecules with four or six transition metals connected via M-Zn-M bridging units resulting in molecular compositions of [{(CO)$_4$Mo}$_4$(Zn)$_6$(μ_2-ZnCp*)$_4$][5] and [Cp*$_2$Rh][(Cp*Rh)$_6$Zn$_6$(ZnCl)$_{12}$(μ_6-Cl)],[6] respectively. Interestingly, these two compounds reveal the fragments {(CO)$_4$MoZn$_4$} and {Cp*RhZn$_4$}, which fulfill the 18 electron rule for M (Zn is treated as one electron ligand). The CO and Cp* ligands that are bound to the starting transition metal gallium complexes can be viewed as spectator ligands or protecting groups at the metal center M. They do not take part in the Cp*/Me ligand exchange reactions at the Ga/Zn sites. From this point of view it is interesting to start a more systematic investigation of the general accessibility and the structural varieties of heteroleptic organozinc-rich compounds of the type [L$_n$M(ZnR)$_5$] (L = nonreactive protecting ligand). For our study presented below, we chose half-sandwich fragments [Cp*M] of iron and ruthenium (M = Fe, Ru; L = Cp*) and their more or less readily available GaCp* complexes as starting materials and targeted so far unknown half-sandwich compounds of the type [Cp*M(ZnR)$_5$], which are expected to be stable and accessible based on the concepts outlined above.

Received: March 27, 2013
Published: May 23, 2013

   dx.doi.org/10.1021/ic400741b | Inorg. Chem. 2013, 52, 7152−7160

RESULTS AND DISCUSSION

1. Synthesis and Structural Characterization of [Cp*Ru(ZnR)$_5$] (1a, 1b, 2a, and 2b). The new complexes [Cp*Ru(ZnCp*)$_3$(ZnMe)(ZnX)] (**1**; **1a**, X = Cl; **1b**, X = Me) and [Cp*Ru(ZnCp*)$_2$(ZnCl)$_3$·THF] (**2a**), whose compositions (see Experimental Section) match with the expected general formula [Cp*Ru(ZnR)$_5$] (R = Cp*, Me, Cl), are formed upon treatment of [Cp*Ru(GaCp*)$_3$Cl] and [Cp*Ru(GaCp*)$_3$][GaCp*Cl$_3$], respectively, with a sufficient amount of six or eight molar equivalents of ZnMe$_2$ to replace all Ga against Zn (Scheme 1).[7] The absence of Ga in **1** and **2a** was

Scheme 1. Synthesis of 1−3

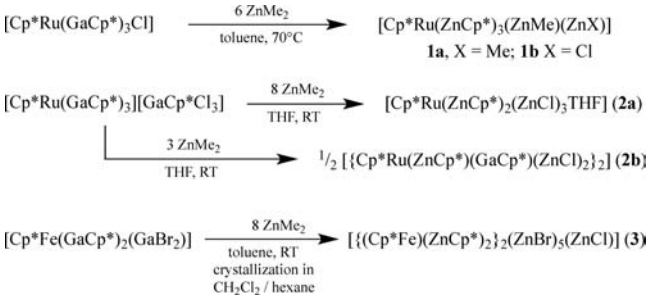

confirmed by atomic absorption spectroscopy. When [Cp*Ru(GaCp*)$_3$][GaCp*Cl$_3$] was treated with only three molar equivalents of ZnMe$_2$ the Ga-containing compound [{Cp*Ru(GaCp*)(ZnCp*)(ZnCl)$_2$}$_2$] (**2b**) was obtained. Whereas **1** was prepared in toluene, the preparation of **2a** and **2b** uses tetrahydrofuran (THF) as the reaction medium of choice because of the ionic nature of the respective starting compound.

[Cp*Ru(ZnCp*)$_3$(ZnMe)(ZnX)] (**1**; **1a**, X = Cl; **1b** X = Me) was characterized by ^{1}H and ^{13}C NMR spectroscopy, elemental analysis, and single crystal X-ray diffraction. Compound **1** is obtained as mixed crystals of [Cp*Ru(ZnCp*)$_3$(ZnMe)(ZnCl)] (**1a**) and [Cp*Ru(ZnCp*)$_3$(ZnMe)$_2$] (**1b**). This is caused by an incomplete Cl/Me exchange reaction, which is obviously highly dependent on the amount of ZnMe$_2$ used. A quantitative Cl/Me exchange cannot be achieved even with prolonged reaction times and higher amounts of ZnMe$_2$. The elemental analysis of representative samples of various crops of **1** reveals an overall Cl/Me ratio of about 4:1 which matches with the integral ratio of the methyl groups compared to the Cp* ligands as obtained by NMR. It was not possible to separate **1a** and **1b** by fractioned crystallization and the crystals obtained consisted of the compound mixture **1** in all cases with an increased amount of **1a**. The ^{1}H NMR spectrum of **1** in C$_6$D$_6$ at 25 °C reveals three resonances in a ratio of 15:5:1.2 with typical chemical shifts for ZnCp*, RuCp*, and ZnMe units, respectively (δ = 2.17, 1.83, and −0.09 ppm). The ZnR (R = Me, Cp*) resonances are both somewhat shifted toward lower field compared to the homoleptic parent compound [Ru(ZnCp*)$_4$(ZnMe)$_6$] (δ = 2.07, −0.19 ppm). Yellow, needle like single crystals were obtained within a few days by cooling a saturated fluorobenzene solution of **1** to −30 °C. Important crystallographic data are summarized in Table 6, and a plot of the molecular structure is shown in Figure 1. Compound **1** crystallizes in the monoclinic space group $P2_1/m$ with **1** containing a crystallographic mirror plane and a cocrystallized fluorobenzene solvent molecule. NMR spectra and elemental

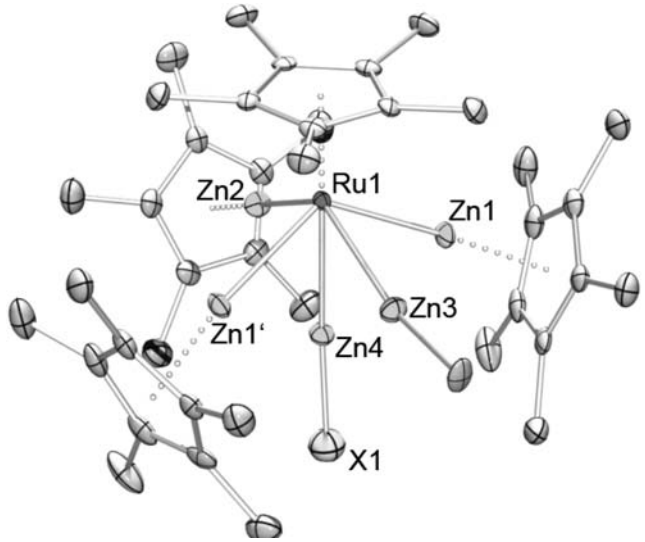

Figure 1. Povray plot of the molecular structure of **1** in the solid state as determined by single crystal X-ray diffraction. The occupancies of X1 were 0.326(3) (**1a**, X1 = Cl) and 0.626(3) (**1b**: X1 = Me). Symmetry-equivalent atoms are generated by a mirror plane, displacement ellipsoids are shown at the 50% probability level, hydrogen atoms as well as cocrystallized solvent molecules have been omitted for clarity. Selected bond length and distances (Å), as well as angles (deg): Ru1−Cp*′$_{centroid}$: 1.879, Ru1−Zn1: 2.495(1), Ru1−Zn2: 2.505(1), Ru1−Zn3: 2.451(1), Ru1−Zn4: 2.463(1), Zn1−Zn2: 3.482, Zn1−Zn3: 2.919, Zn1−Zn4: 2.677(1), Zn2−Zn4: 2.621(1), Zn3−Zn4: 2.828(1), Zn1−Cp*$_{centroid}$: 2.012, Zn2−Cp*$_{centroid}$: 2.000, Zn3-Me: 1.990(6), Zn4-X1: 2.069(4), Ru1−Zn1−Cp*$_{centroid}$: 167.16, Ru1−Zn2−Cp*$_{centroid}$: 179.56, Ru1−Zn3−Cp*$_{centroid}$: 163.17, Ru1−Zn1−Zn4: 56.75(2), Ru1−Zn2−Zn4: 57.41(2), Ru1−Zn3−Zn4: 55.08(2), Ru1−Zn4-X1: 175.0(1).

analysis yielded a 4:1 ratio of **1a**/**1b** for the bulk sample, whereas refinement of the occupancies yielded a ratio of 0.326(3)/0.674(3) for **1a** and **1b** in the selected crystal which was used for the structure determination of **1**.

The Ru center of **1** is surrounded by one η^5-Cp* ligand as well as five ZnR (R = Cp*, Me, X) groups. The ZnCp* groups result from the Ga/Zn and Cp*/Me exchange outlined in the introduction. Taking the Cp* as one coordination site, one may describe the resulting structure as highly distorted octahedral. The ZnX ligand is located in the axial position of the square pyramidal {Ru(ZnR)$_5$} unit, while the ZnCp* and ZnMe ligands occupy the equatorial positions. The preference of the equatorial position of the ZnCp* may be for steric reasons. All Zn-R (R = Cp*, Me) and Ru−Zn bond lengths are quite comparable to those found in [Ru(ZnCp*)$_4$(ZnMe)$_6$] and do not show any deviations from expected values. Additionally the obtained Ru−Zn distances compare well to the data known for Ru/Zn solid state phases such as RuZn$_3$, which contain a cuboctahedral RuZn$_{12}$ structure with somewhat longer Ru−Zn distances of 2.624(1) and 2.791(1) Å because of the higher coordination number.[8] The Zn−Zn contacts of **1** are much longer than in [Zn$_2$Cp*$_2$][9] with a Zn−Zn distance of 2.305(3) Å and slightly longer compared to the Ru/Zn solid state phase RuZn$_3$ with Zn−Zn distances of 2.665(1)−2.749(1) Å, whose comparison clearly indicates the absence of significant covalent bonding characteristics.[8]

The treatment of the salt [Cp*Ru(GaCp*)$_3$][GaCp*Cl$_3$] with the full stoichiometric amount of ZnMe$_2$ (8 molar equiv) for achieving a complete Ga/Zn exchange in THF affords

dx.doi.org/10.1021/ic400741b | Inorg. Chem. 2013, 52, 7152−7160

compound [Cp*Ru(ZnCp*)$_2$(ZnCl)$_3$·THF] (**2a**) (Scheme 1) in the form of yellow cubic shaped crystals. The ^{1}H NMR spectrum of **2a** in C_6D_6 at room temperature exhibits the expected resonances at δ = 3.57 and 1.40 ppm for the THF moiety. Three additional resonances with an integral ratio of 1:1:1 at δ = 2.23, 2.16, and 1.81 ppm are observed. This signal pattern is assigned to two different ZnCp* units, which are not equivalent on the NMR time scale. This is certainly caused by the "static" non symmetric nature of the molecule, that is, neither ZnR ligands nor the coordination of the THF molecule is dynamic on the NMR time scale. Several attempts (various solvents and crystallization techniques) failed to obtain good single crystals of **2a**. Nevertheless we were able to determine and confirm the connectivity of the severely disordered molecular structure of **2a** with a distorted pentagonal-pyramidal environment around the central Ru atom (similar to Fe2 in **3**). One THF molecule is attached to one ZnCl moiety (and is disordered), which therefore leads to three different Cp* resonances in the NMR spectrum. Because of the poor quality of the obtained structural data we do not present these and do not provide a more detailed discussion.

Interestingly, the reaction of [Cp*Ru(GaCp*)$_3$][GaCp*Cl$_3$] with a smaller amount of ZnMe$_2$ (3 molar equiv) leads to the formation of the Ga-containing dimer [{Cp*Ru(GaCp*)-(ZnCp*)(ZnCl)$_2$}$_2$] (**2b**). Similar reactions with less than stochiometric amounts of ZnMe$_2$ (for a full Ga/Zn exchange) lead to related M/Zn/Ga metal mixed compounds, which have been reported previously (i.e., [Mo(GaMe)$_4$(ZnCp*)$_4$] and [Mo(GaMe)$_2$(ZnCp*)$_4$(ZnMe)$_4$]).[3] The ^{1}H NMR spectrum of **2b** shows three individual resonances in the region typical for Cp* ligands at 2.27, 1.87, and 1.84 ppm, with an integral ratio of 1:1:1, clearly indicating three types of Cp* ligands. The ^{13}C NMR data confirm the presence of three distinct Cp* ligands with two resonances for each Cp* ligand. A plot of the molecular structure of **2b** is depicted in Figure 2. **2b** crystallizes in the monoclinic space group $P2_1/c$ residing on a crystallographic inversion center. The molecular structure of **2b** consists of two distorted square pyramidal units [Cp*Ru(GaCp*)-(ZnR)$_3$] (R = Cp*, Cl, μ_2-Cl) with Cp* in the axial, and the four other GaR and ZnR (R = Cp*, Me, Cl) moieties in the equatorial position around the Ru center. The two fragments [Cp*Ru(M′R)$_4$] (M′ = Ga, Zn) are connected by a planar, bridging Zn(μ_2-Cl)$_2$Zn motif which features a three coordinate Zn. This motif is quite rare but some complexes like [Ar′Zn(μ_2-I)$_2$ZnAr′] (Ar′ = C$_6$H$_3$-2,6-(C$_6$H$_3$-2,6-Pr$^i_2$)$_2$) are known, which are also arranged as a Lewis acid base pair in the solid state.[10] The units RuCp*, ZnCp*, and GaCp* of each fragment are located in trans position to each other (center of inversion in the central Zn(μ_2-Cl)$_2$Zn unit). Compound **2b** can be understood as a Lewis acid base pair of [Cp*Ru(GaCp*)-(ZnCp*)(ZnCl)$_2$] (18 valence electrons at Ru) which is quite similar to the previously reported dimer of [Cp*Rh-(ZnCp*)$_2$(ZnMe)(ZnCl)] (18 valence electrons at Rh).[6] The Ru−Zn bond lengths vary between 2.404(1)−2.486(1) Å and are substantially shorter than in the homoleptic parent complex [Ru(ZnCp*)$_4$(ZnMe)$_6$] (a.v. 2.521 Å).

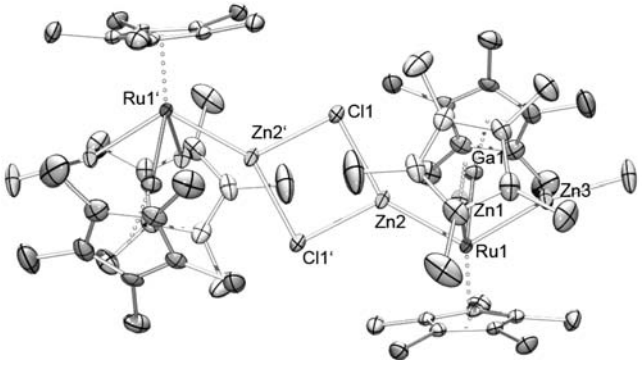

Figure 2. Povray plot of the molecular structure of **2b** in the solid state as determined by single crystal X-ray diffraction. Symmetry-equivalent atoms are generated by a center of inversion, displacement ellipsoids are shown at the 50% probability level, hydrogen atoms have been omitted for clarity. Selected bond length and distances (Å), as well as angles (deg): Ru1−Cp*$_{centroid}$: 1.846, Zn1−Cp*$_{centroid}$: 1.977, Ga1−Cp*$_{centroid}$: 1.950, Ru1−Zn1: 2.486(1), Ru1−Zn2: 2.448(1), Ru1−Zn3: 2.404(1), Ru1−Ga1: 2.362(1), Zn1−Zn2: 2.687(1), Zn1−Zn3: 2.706(1), Ga1−Zn2: 3.113, Ga1−Zn3: 2.931(1), Zn2−Cl1: 2.357(1), Zn2−Cl1′: 2.424(1), Zn3−Cl2: 2.169(1), Cp*$_{centroid}$−Zn1−Ru1: 171.99, Cp*$_{centroid}$−Ga1−Ru1: 172.03.

The assignment of Ga and Zn in the molecular structures of the compounds discussed cannot be unambiguously performed based on routine single crystal X-ray diffraction and refinement data, since the scattering properties of Zn and Ga are equal. In many complexes with mixed ZnR/GaR ligands such as [Rh(GaMe)(ZnCp*)$_4$(ZnMe)$_3$] or [Mo-(GaMe)$_2$(ZnCp*)$_4$(ZnMe)$_4$] no significant differences between the various M-Zn/Ga and Zn/Ga-R distances can be observed, since the Ga atom(s) are distributed throughout various positions leading to averaged values of the corresponding distances during the structure refinement. ^{1}H NMR studies and especially high or low temperature NMR measurements can help to assign the organic ligand attached to the corresponding Zn or Ga atom, but this type of analysis certainly does not provide a definite answer. Neutron diffraction data or resonant X-ray diffraction techniques might help, but were unavailable for this work. Nevertheless, based on a careful comparison of the metal−metal bond lengths of **2b** with the data set of known structures of this family of compounds we can support our assignment: The four M′R ligands (M′ = Ga, Zn; R = Cp*, Cl) in the equatorial plane of the square pyramidal environment of the Ru center (ZnCp*, GaCp*, ZnCl$_{terminal}$, ZnCl$_{bridging}$) show rather different M′-M′ distances. The two very short distances of 2.687(1) and 2.706(1) Å are comparable to the weakly attractive tangential Zn−Zn interactions in the homoleptic reference compound [Ru(ZnCp*)$_4$(ZnMe)$_6$] (a.v. 2.80 Å), whereas the two characteristically longer distances of 3.113(1) and 2.931(1) Å are indicative of Zn···Ga distances. This assignment is in good agreement with the Ru-M′ bond lengths. They are significantly longer for Ru−Zn (a.v. 2.45 Å) than for Ru−Ga (2.362(1) Å). These values fit well to the reference data for other Ru/Ga and Ru/Zn reference complexes, such as [Ru-(PCy$_3$)$_2$(GaCp*)$_2$(H)$_2$] (Ru−Ga: a.v. 2.401(1) Å),[11] [Ru-(η^2,η^2-COD)(GaCp*)$_3$] (Ru−Ga: a.v. = 2.375 Å)[12] (COD = 1,5-cyclooctadiene), [Ru(TMM)(ZnCp*)$_3$(ZnMe)$_3$] (Ru−Zn: a.v. 2.48 Å)[13] (TMM = trimethylenemethane), and homoleptic [Ru(ZnCp*)$_4$(ZnMe)$_6$] (Ru−Zn: a.v. 2.521 Å). Interestingly the respective comparison of the Zn/Ga-R distances do not seem to follow a certain trend: Whereupon the Zn−Cp* distances in **2b** of 1.977 Å are almost equal to the parent complex [Ru(ZnCp*)$_4$(ZnMe)$_6$] (Zn−Cp*$_{centroid}$: a.v. 1.97 Å) and the corresponding Ga−Cp* distances 1.951 Å are similar compared to complexes like [Ru(PCy$_3$)$_2$(GaCp*)$_2$(H)$_2$] (Ga−

dx.doi.org/10.1021/ic400741b | Inorg. Chem. 2013, 52, 7152−7160

$Cp^*_{centroid}$: a.v. 2.05 Å)[11] or [Ru(η^2,η^2-COD)($GaCp^*)_3$] (a.v. = 2.00 Å).[12]

2. Synthesis and Structural Characterization of [{(Cp*Fe)(ZnCp*)$_2$}$_2$(ZnBr)$_5$(ZnCl)] (3). In a similar manner as described for **1**, **2a**, and **2b** the treatment of [Cp*Fe($GaCp^*)_2$($GaBr_2$)][14] with 8 equiv of $ZnMe_2$ gave the complex [{(Cp*Fe)($ZnCp^*)_2$}$_2$($ZnBr)_5$(ZnCl)] (**3**) (Scheme 1). The absence of gallium in **3** was also confirmed by atomic absorption spectroscopy. Compound **3** crystallized in dark-red block-shaped single crystals upon slow diffusion of hexane into a saturated solution in dichloromethane at room temperature. Because of the need of a polar solvent like CH_2Cl_2 for the crystallization of **3**, a Cl/Br exchange occurred and one Cl atom was found to be located at one of the Zn sites, exclusively. This halide exchange is not unusual when using CH_2Cl_2 as a solvent.[15] Important crystallographic data of **3** are summarized in Table 6, and a plot of the molecular structure is depicted in Figure 3. Compound **3** crystallizes in the monoclinic space group *C*2/*c* as a dichloromethane solvate hexane hemisolvate.

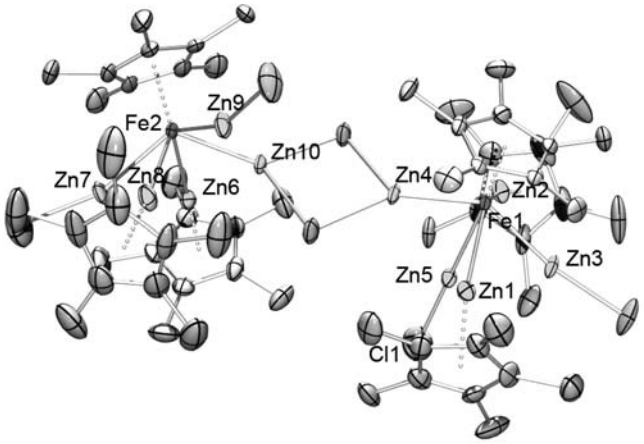

Figure 3. Povray plot of the molecular structure of **3** in the solid state as determined by single crystal X-ray diffraction. Symmetry-equivalent atoms are generated by a center of inversion, displacement ellipsoids are shown at the 50% probability level, hydrogen atoms have been omitted for clarity. Selected bond lengths and angles are summarized in Table 1.

Table 1. Selected Average Bond Lengths (Å) and Angles (deg) of 3

octahedral unit		pentagonal pyramidal unit	
Fe1−Zn	2.383	Fe2−Zn	2.415
Fe1−$Cp^*_{centroid}$	1.728	Fe2−$Cp^*_{centroid}$	1.737
Zn−Zn	2.734	Zn−Zn	2.560
Zn−$Cp^*_{centroid}$	1.977	Zn−$Cp^*_{centroid}$	1.943
Fe1−Zn−$Cp_{centroid}$	171.7	Fe2−Zn−$Cp^*_{centroid}$	176.5
$Cp^*_{centroid}$−Fe1−Zn5	173.9		

Compound **3** is best regarded as a Lewis acid/base adduct of two fragments {Cp*FeZn$_5$}, which are bridged by two Br atoms forming a Zn(μ-Br)$_2$Zn moiety, which situation is quite similar to **2b**. However, in contrast to **2b** the two fragments {Cp*FeZn$_5$} adopt different coordination geometries in one molecule. While one {Cp*FeZn$_5$} unit shows an octahedral arrangement around Fe1 similar to **1**, the second unit reveals an even more distorted pentagonal pyramidal coordination sphere of Fe2, as suggested for **2a**, but without a coordinating THF molecule. The Fe−Zn bond lengths vary between 2.314(1) and 2.486(2) Å and are shortened compared to other Fe/Zn mixed compounds like [$(CO)_3$Fe{μ_2-Zn($THF)_2$}$_2$(μ_2-$ZnMe)_2$Fe-$(CO)_3$][16] (Fe-ZnMe: 2.464(2)−2.563(1) Å). Although the atoms in **3** are arranged in a way to give a highly asymmetric environment in the solid state structure, only two resonances for the Cp* ligands are present in the ^{1}H NMR spectrum in dichloromethane solution at 26 °C with an integration ratio of 2:1. This effect may be caused either by a fast fluxional behavior of the Cp* ligands on the NMR time scale (even at −80 °C), or a different molecular connectivity in solution than in the solid state (probably a monomer/dimer equilibrium). Nevertheless the chemical shifts of 2.07 and 1.97 ppm can be easily assigned to ZnCp* and FeCp* units, respectively. This is in good agreement to [Ru($ZnCp^*)_4$($ZnMe)_6$] (2.07 ppm) and [Cp*Fe($GaCp^*)_2$($GaBr_2$)] (1.77 ppm), although the FeCp* resonance is significantly shifted to higher field.

3. Comparison of [Cp*MZn$_5$] Fragments with Continuous Shape Measure Analysis (CShM). The Cartesian coordinates of all structures used in the discussion below can be found in the Supporting Information. The method of choice for the comparison of two polyhedra is the continuous shape measure (CShM).[3,17] In this procedure, N_Q vertices of one polyhedron are given by their position vectors $\vec{Q}_i$ (i = 1, 2, 3 ..., N_Q), as well as N_P vertices of a second polyhedron with the position vectors $\vec{P}_i$ (i = 1, 2, 3 ..., N_P). The smallest distance S_Q(P) of the position vectors between both polyhedra can be calculated with the eq 1 and the constraint $N = N_Q$ if $N_P > N_Q$, otherwise $N = N_P$. The continuous shape measure calculation previously used by us was designed for polyhedra with an equal number of edges;[3] in this particular study we were interested in the comparison of two polyhedra with an unequal number of edges. Here a Cp* ligand is substituted in principle by five ZnR units also giving an 18 VE complex as nicely depicted in Figure 4 below.

$$S_Q(P) = \frac{1}{N}\min \sum_{i=1}^{N} |\vec{Q}_i - \vec{P}_i|^2 \times 100 \quad (1)$$

The comparison of a five edged half polyhedral arrangement and homoleptic 10-fold ZnR ligated transition metal center was utilized. Prior to all comparisons all analyzed polyhedra were centered at the origin and were normalized. We have described the details of our approach to compute the S_Q(P) values previously.[3] The final values for S_Q(P) vary between 0 and 100 and serve as a quantitative measure. With S_Q(P) = 0, the polyhedron represents the exact overlap of both polyhedra, while increasing values denote increasing distortions. Table 2 gives a summary of the S_Q(P) values for the new half-sandwich complexes [Cp*M($ZnR)_5$] with a comparison of experimental and calculated structures (see the DFT section below). According to our results those of Alvarez et al., who performed extensive studies on the structures of various highly coordinated metal complexes, shape measures S_Q(P) below 1.0 indicate minor, non significant distortions, while values of 1.0 < S_Q(P) < 3.0 indicate important, significant distortions between both polyhedrons, however, still providing a suitable description.[18] As we have previously reported twelve, nine, and eight coordinated transition metal ZnR stabilized compounds are almost perfectly arranged in an ideally shaped manner. In contrast, the 10-fold coordinated compounds show major distortions from ideal shapes.[19] At first glance only three S_Q(P) values in Table 2 match the criteria of minor distortions which

dx.doi.org/10.1021/ic400741b | Inorg. Chem. 2013, 52, 7152−7160

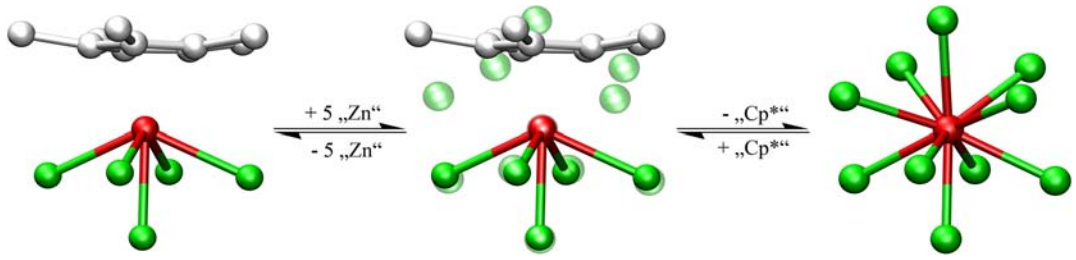

Figure 4. Superimposition (center) of a $[Cp^*MZn_5]$ fragment (left) and a $[MZn_{10}]$ unit (right); red: d^8 transition metal, green: Zn, white: C.

Table 2. Continuous Shape Measures (CShM) of Various Polyhedra and Compounds (1 and 3)

compound	$[Ru(ZnCp^*)_4(ZnMe)_6$	4A,6B-extended dodecahedron	VGa_{10} solid state structure[a]	Bicapped-square antiprism
(1)	0.49	1.31	0.96	1.96
(3) Fe1	0.5	1.09	1.22	2.10
(3) Fe2	3.90	3.72	3.07	4.77

[a] VGa_{10} coordination polyhedron extracted from the solid state structure of V_8Ga_{41} has been used as a model for a centaur polyhedron (half-cube half-icosahedron).[20]

strongly underlines the more or less problematic character of 10-fold coordinated complexes. But the shape measure clearly shows best congruence if compared to a so-called centaur polyhedron. This body has been extracted from the solid state structure of V_8Ga_{41} which has been used as a model constructed by fusing two ideal polyhedra to form one 10-fold body, for example, one cube and one icosahedron.[20] A "simple" substitution of five ZnR units from $[Ru(ZnCp^*)_4(ZnMe)_6]$ by one Cp* ligand can only be performed in the almost octahedrally coordinated (Cp* taken as one 5 electron ligand position) compounds **1** and **3** (Fe1) giving $S_Q(P)$ values of about 0.5. The nearly pentagonal pyramidal arranged polyhedron in **3** (Fe2) shows best congruence to the solid state structure of VGa_{10}.

4. Computational Investigations on the Bonding Situation in $[Cp^*Ru(ZnR)_5]$. In this study we were interested in the comparison of the bonding situation of the reference compounds $[Ru(ZnCp^*)_4(ZnMe)_6]$ (pseudo homoleptic) with their heteroleptic derivatives $[Cp^*Ru(ZnR)_5]$ (**1**, R = Cp*, CH_3, Cl) which feature a Cp* ligand attached directly to the transition metal leading to a decreased number of ZnR ligands arranged around the central metal atom. The electronic structures of the systems $[Cp^*Ru(ZnCp^*)_3(ZnMe)(ZnX)]$ (**1**; **1a**, X = Cl; **1b** X = Me) and $[Ru(ZnCp^*)_4(ZnMe)_6]$ as well as of the model systems $[Cp^*Ru(ZnCl)_5]$, $[Cp^*Ru(ZnMe)_5]$, $[Ru(ZnCl)_{10}]$, and $[Ru(ZnMe)_{10}]$ were investigated by using several theoretical tools (NBO charges, AIM, EDA-NOCV) at the BP86/TZVPP level of theory, to get an insight into the bonding situation of these systems. A comparison of the calculated structures with the experimentally derived molecular data shows that the most important bond lengths of the DFT-optimized molecules are predicted up to 0.05 Å longer, the exception of ZnCp ligands where the deviation is up to 0.07 Å. This effect can be explained by the occurring bond shortening in the solid state compared to the gas phase environment in the calculations.

The calculated NBO partial charges give a clearly negatively charged Ru atom (−1.39e in $[Cp^*Ru(ZnCp^*)_3(ZnMe)(ZnCl)]$ (**1a**) and −2.66e in $[Ru(ZnCp^*)_4(ZnMe)_6]$), while the ZnR ligands are fairly positive (≈ 0.33e for R = Me, Cl and ≈0.15e for R = Cp*). The Cp* ligand at the Ru atom in $[Cp^*Ru(ZnCp^*)_3(ZnMe)(ZnCl)]$ (**1a**) is predicted as slightly negative. In the EDA-NOCV (results see Tables 3−5) two

Table 3. EDA-NOCV results (BP86/TZ2P+) in kcal/mol for $[Cp^*Ru(ZnMe)_5]$[a] and $[Ru(ZnMe)_{10}]$[b]

	$[Cp^*Ru(ZnMe)_5]$	$[Ru(ZnMe)_{10}]$
ΔE_{int}	−839.5	−882.1
ΔE_{Pauli}	1021.3	925.4
ΔE_{elstat}	−1407.0 (75.6%)	−1496.2 (82.8%)
ΔE_{orb}	−453.9 (24.4%)	−311.4 (17.2%)

[a] Occupation of fragments: Ru^{2-}, singlet ($s^0p^0d^{10}$); $[Cp^*\text{-}(ZnMe)_5]^{2+}$, singlet. [b] Occupation of the fragments: Ru^{2-}, singlet ($s^0p^0d^{10}$); $[(ZnMe)_{10}]^{2+}$, singlet.

fragmentation schemes were investigated: First, the interaction of the Ru atom with the surrounding ligand. The best description for the fragment occupation (values for ΔE_{orb} closest to zero) was achieved with Ru^{2-} in s^0d^{10} and the corresponding ligand cage in a singlet configuration. Additionally, the interaction energies for the different ligand types were calculated; here, the ZnR ligands were treated as doublet fragments and Cp* as anions in a singlet state. Because of the increased system size when Cp* is involved, model compounds, where only ZnMe ligands are present, were investigated by the means of the EDA-NOCV to get an insight into the bonding situation between the ruthenium atom and all other ligands. In the analysis of the interaction of Ru and one type of ligand the following systems were considered to get information about the specific ligand types: For ZnCl and ZnMe the model systems $[Cp^*Ru(ZnCl)_5]$, $[Cp^*Ru(ZnMe)_5]$, $[Ru(ZnCl)_{10}]$, and $[Ru(ZnMe)_{10}]$ were taken into account, while the synthesized molecules $[Cp^*Ru(ZnCp^*)_3(ZnMe)(ZnX)]$ (**1**; **1a**, X = Cl; **1b** X = Me) and $[Ru(ZnCp^*)_4(ZnMe)_6]$ were analyzed to extract information about the bond between Ru and Cp* respectively ZnCp*. The intrinsic interaction energy ΔE_{int} between Ru^{2-} and the ligands in $[Cp^*Ru(ZnMe)_5]$ is −839.5 kcal/mol (Table 3, deformation densities can be found in the Supporting Information), where about 75% of this is due to electrostatic interaction (ΔE_{elstat}).

With the help of the deformation densities, the orbital interaction (ΔE_{orb}) could be divided into different components, which correspond to the occupied d-orbitals of Ru^{2-}. The main contributions (−170.1 kcal/mol, each) arise from d_{xz} and d_{yz} orbitals, which are orthogonal with respect to the Cp* ring of the ruthenium atom. It is visible that the upper lobes of these

dx.doi.org/10.1021/ic400741b | Inorg. Chem. 2013, 52, 7152−7160

orbitals strongly overlap with the π-system of Cp*. The deformation densities clearly show that electron density is donated from ruthenium to the Cp* ligand to create a bond between them. The second highest contribution to ΔE_{orb} is the interaction between the d_{z^2} orbital and the surrounding ligands: Here, electron density from the ruthenium as well as from the Cp* ring is used to bind to the ZnMe ligands. The contributions of the d_{xy} and $d_{x^2-y^2}$ orbitals, which are parallel with respect to the Cp* ring, are the smallest. The electrons of ruthenium are donated partly into bonds between Ru and Cp* and partly into bonds between Ru and the ZnR ligands. A comparison between the different ligand types shows that the ligand bond strengths follow the order Cp* (−210.6 kcal/mol) > ZnCl (−84.0 kcal/mol) > ZnMe (−79.9 kcal/mol) > ZnCp* (−65.1 kcal/mol). The bond lengths between ruthenium and the ligands correspond to this trend: with increasing bond strengths, the calculated bond lengths are decreasing.

The intrinsic interaction energy between ruthenium and the other ligands in $[Ru(ZnMe)_{10}]$ (−882.1 kcal/mol) is slightly higher compared to $[Cp^*Ru(ZnMe)_5]$, but the orbital contribution is significantly lower (−311.4 kcal/mol compared to −453.9 kcal/mol in $[Cp^*Ru(ZnMe)_5]$), which can be explained by the deformation densities (provided in the Supporting Information): while there were two very strong contributions between ruthenium and the Cp* ligand due to the good overlap between d-orbitals and π-system in $[Cp^*Ru(ZnMe)_5]$, this can not be found in $[Ru(ZnMe)_{10}]$. Here, the strongest contribution is the donation of electrons from the d_{z^2} orbital of ruthenium toward the orbital oriented ZnMe ligands. The other contributions are of similar strengths (around −67 kcal/mol), as no other especially favorable orientations of the d-orbitals toward the ligands appear in this system. The bond strengths of each of the different ZnR ligands in $[Ru(ZnR)_{10}]$ are almost the same compared with each other (Tables 4, 5).

Table 4. Comparison between EDA-NOCV Results of the Different $[Cp^*Ru(ZnR)_5]$ Systems in kcal/mol[a]

	ZnCl[b]	ZnMe[c]	ZnCp*[d]	Cp*[e]
ΔE_{int}	−84.0	−79.9	−65.1	−210.6
ΔE_{Pauli}	189.7	299.0	160.6	291.7
ΔE_{elstat}	−155.4 (56.8%)	−158.4 (41.8%)	−142.9 (63.4%)	−289.4 (57.6%)
ΔE_{orb}	−118.2 (43.2%)	−220.5 (58.2%)	−82.7 (36.7%)	−212.9 (42.4%)

[a]Occupation of the fragments see footnotes *b*–*e*. [b]$[Cp^*Ru(ZnCl)_5]$: ZnCl, doublet ; $Cp^*Ru(ZnCl)_4$, doublet. [c]$[Cp^*Ru(ZnMe)_5]$: ZnMe, doublet ; $Cp^*Ru(ZnMe)_4$, doublet. [d]$[Cp^*Ru(ZnCp^*)_2(ZnMe)(ZnCl)]$: ZnCp*, double ; $[Cp^*Ru(ZnCp^*)(ZnMe)(ZnCl)]$, doublet. [e]$[Cp^*Ru(ZnCp^*)_2(ZnMe)(ZnCl)]$: Cp^{*-}, singlet; $[Ru(ZnCp^*)_2(ZnMe)(ZnCl)]^+$, singlet.

By means of the QTAIM, molecular graphs and Laplacians of the electron densities were calculated: bond paths could only be found between ruthenium and the surrounding ligands. The shape of the Laplacian and the absence of bond paths lead to the conclusion that the zinc atoms do not strongly interact with each other[39] and the systems can be best described as classical complexes, where the bonds are formed in a donor–acceptor like fashion between the d-electrons of ruthenium and the surrounding ligands (Figure 5).

Table 5. Comparison between EDA-NOCV Results of the Different $[Ru(ZnR)_{10}]$ Systems in kcal/mol[a]

	ZnCl[b]	ZnMe[c]	ZnCp*[d]
ΔE_{int}	−70.0	−69.4	−70.6
ΔE_{Pauli}	153.4	201.2	181.0
ΔE_{elstat}	−122.2 (54.7%)	−176.5 (65.2%)	−161.4 (64.1%)
ΔE_{orb}	−101.3 (45.3%)	−94.1 (34.8%)	−90.3 (35.9%)

[a]Occupation of the fragments see footnotes *b*–*d*. [b]$[Ru(ZnCl)_{10}]$: ZnCl, doublet ; $Ru(ZnCl)_9$, doublet. [c]$[Ru(ZnMe)_{10}]$: ZnMe, doublet ; $Ru(ZnMe)_9$,doublet. [d]$[Ru(ZnCp^*)_4(ZnMe)_6]$: ZnCp*, doublet; $[Ru(ZnCp^*)_3(ZnMe)_6]$, doublet.

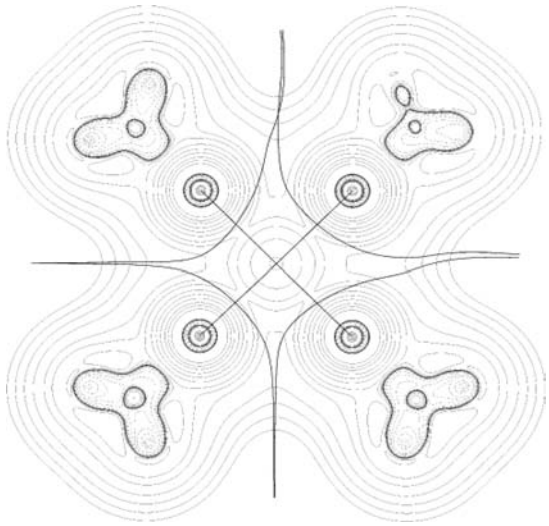

Figure 5. Molecular graph and contour map of the Laplacian within the Zn1–Zn2–Zn3–Zn4 plane of $[Cp^*Ru(ZnMe)_5]$ (BP86/TZVPP).

CONCLUSION

Obviously, the coordination geometry of the central metal in such zinc-rich complexes is not only determined by the electron count of the transition metal, but the influence of nonrepulsive or even weakly attractive ligand–ligand interaction is also affecting the distribution of the ligands around the central atom. Indeed, this seems to be the case also for all-metal coordinated compounds such as the homoleptic $[M(ZnR)_n]$ or heteroleptic $[M(ZnR)_n(GaR)_m]$, which adopt ideal platonic bodies in all cases independent of the electron count of the central metal M. However, the results of this work point to the fact that the structures of heteroleptic metal-rich compounds $[Cp^*M(ZnR)_5]$ (M = Fe, Ru) are not easily deducible from the electronic nature of the central metal as in classical coordination compounds, but require a deeper understanding of the electronic structure of the whole metal core, as in metal cluster compounds.

EXPERIMENTAL SECTION

Synthesis Protocols, General Preparative and Spectroscopic Methods. All manipulations were carried out in an atmosphere of purified argon using standard Schlenk and glovebox techniques. Hexane, toluene, and THF were dried using a MBraun Solvent Purification System. Fluorobenzene was dried over an alumina column and stored under argon atmosphere. The final H_2O content in all solvents was checked by Karl Fischer titration and did not exceed 5 ppm. $[Cp^*Ru(GaCp^*)_3Cl]$, $[Ru(GaCp^*)_3][GaCp^*Cl_3]$[7] and $[Cp^*Fe(GaCp^*)_2(GaBr_2)]$[14] were prepared according to recent literature methods. CHN microanalyses were carried out with a

dx.doi.org/10.1021/ic400741b | Inorg. Chem. 2013, 52, 7152–7160

Table 6. Crystallographic Data and Refinement Details for 1, 2b, and 3·CH_2Cl_2·0.5C_6H_{14}

	1·C_6H_5F	2b	3·CH_2Cl_2·0.5C_6H_{14}
empirical formula	$C_{47.67}H_{69.35}Cl_{0.33}FRuZn_5$	$C_{60}H_{90}Cl_4Ga_2Ru_2Zn_6$	$C_{64}H_{99}Br_5Cl_3Fe_2Zn_{10}$
M_r	1101.04	1686.92	2139.73
T (K)	113(2)	113(2)	113(2)
crystal size (mm^3)	0.20 × 0.15 × 0.10	0.20 × 0.20 × 0.10	0.40 × 0.30 × 0.30
crystal system	monoclinic	monoclinic	monoclinic
space group	$P2_1/m$	$P2_1/c$	$C2/c$
a (Å)	9.8706(2)	16.1517(6)	46.3667(14)
b (Å)	17.3390(3)	11.6946(4)	12.3619(2)
c (Å)	13.7515(3)	18.4912(7)	30.976(1)
α (Å)	90	90	90
β (Å)	96.198(2)	104.974(4)	119.465(4)
γ (Å)	90	90	90
V ($Å^{-3}$)	2339.76(8)	3374.2(2)	15458.1(7)
Z	2	2	8
ρ_{calc} (mg m^{-3})	1.563	1.660	1.839
μ (mm^{-1})	2.890	3.503	6.128
θ range (deg)	2.98−25.00	2.90−26.50	2.93−25.00
completeness to θ_{max} (%)	99.8	99.7	98.1
reflections collected/unique	8151/4267	12814/6987	39163/13371
observed reflections [$I > 2\sigma(I)$]	3336	5655	9983
R_{int}	0.0211	0.0267	0.0206
parameters/restraints	302/30	349/0	733/0
goodness-of-fit on F^2	0.904	1.019	1.072
R_1 [$I > 2\sigma(I)$]	0.0231	0.0289	0.0433
wR_2 (all data)	0.0496	0.0686	0.1386
residuals (e $Å^{-3}$)	0.491/−0.526	0.828/−0.609	1.420/−2.707

Vario EL elemental analyzer. Zinc and gallium contents were determined by atomic absorption spectroscopy. NMR spectra were recorded on a Bruker Avance DPX-250 spectrometer (^{1}H, 250.1 MHz; ^{13}C, 62.9 MHz) in either C_6D_6 or CD_2Cl_2 at 298 K. Chemical shifts are given relative to TMS and were referenced to the solvent resonances as internal standards. The chemical shifts are described in parts per million (ppm), downfield shifted from TMS and are consecutively reported as position (δH and δC), relative integral, multiplicity (s = singlet, m = multiplet), coupling constant (J in Hz) and assignment.

*[Cp*Ru(ZnCp*)$_3$(ZnMe)(ZnX)] (**1**; **1a**, X = Cl; **1b** X = Me).* A suspension of [Cp*Ru(GaCp*)$_3$Cl] (85 mg, 0.096 mmol) in toluene (5 mL) was treated with 2 M $ZnMe_2$ (5 equiv, 0.24 mL, 0.48 mmol) at −30 °C, then warmed up to 70 °C and stirred for 30 min. After filtration the filtrate was dried in vacuo and recrystallized from fluorobenzene at −30 °C within a few days. Yield: 0.054 g (55%). ^{1}H NMR (250.1 MHz, C_6D_6, 24 °C): δ = 2.17 (s, 45H, ZnCp*), 1.83 (s, 15H, RuCp*), −0.09 (s, 3.6 H, ZnMe) ppm. ^{13}C NMR (62.9 MHz, C_6D_6, 24 °C): δ = 112.9 100.6, 15.8, 11.7, 11.6 ppm. Note: Compound **1** is obtained as a mixture of **1a** (80%), X = Cl and **1b** (20%), X = CH_3. See the discussion in the main text. Elemental analytic data (dried sample) calc. for $RuZn_5Cl_{0.8}C_{41.2}H_{63.6}$ (determined by NMR): C, 48.2; H, 6.3; Zn, 32.3; found: C, 48.1; H, 6.4; Zn, 31.8, no gallium was detected.

*[Cp*Ru(ZnCp*)$_2$(ZnCl)$_3$·THF] (**2a**).* A solution of [Ru(GaCp*)$_3$]-[GaCp*Cl$_3$] (125 mg, 0.107 mmol) in THF (5 mL) was treated with 2 M $ZnMe_2$ (8 equiv, 0.43 mL, 0.86 mmol) at −30 °C, warmed to room temperature (RT) and stirred for 30 min. After extraction out of hexane and drying in vacuo, suitable single-crystals could be obtained within a few days out of a solution in THF stored at −30 °C. Yield: 0.045 (42%). ^{1}H NMR (250.1 MHz, C_6D_6, 24 °C): δ = 3.57 (m, 4H, THF), 2.23 (s, 15H, ZnCp*), 2.16 (s, 15H, ZnCp*), 1.81 (s, 15H, RuCp*), 1.40 (m, 4H, THF) ppm. ^{13}C NMR (62.9 MHz, C_6D_6, 24 °C): δ = 112.4 100.8, 68.6 (THF), 24.2 (THF), 15.6, 11.2 ppm. Elemental analytic data (dried sample in vacuo) calc. for $RuZn_5Cl_3OC_{34}H_{53}$: C, 40.3; H, 5.3; Zn, 32.3; found: C, 40.5; H, 5.1; Zn, 32.0, no gallium was detected.

*[{Cp*Ru(ZnCp*)(GaCp*)(ZnCl)(Znμ_2-Cl)}$_2$] (**2b**).* Compound **3** was prepared like **2** by using 6 mol equiv of $ZnMe_2$ instead of 8 mol equiv. Yield: (65%). ^{1}H NMR (250.1 MHz, C_6D_6, 24 °C): δ = 2.27 (s, 15H, GaCp*), 1.87 (s, 15H,ZnCp*), 1.84 (s,15H, RuCp*) ppm. ^{13}C NMR (62.9 MHz, C_6D_6, 24 °C): δ = 140.5 (s, GaC_5Me_5), 110.9 (s, ZnC_5Me_5), 100.4 (s, RuC_5Me_5), 16.3 (s, RuC_5Me_5), 11.4 (GaC_5Me_5), 10.1 (s, ZnC_5Me_5) ppm. Elemental analytic data (dried sample in vacuo) calc. for $Ru_2Ga_2Zn_6Cl_4C_{60}H_{90}$: C, 42.7; H, 5.4; Zn, 23.3; Ga, 8.3; found: C, 42.4; H, 5.2; Zn, 23.1; Ga, 8.1.

*[{(Cp*Fe)(ZnCp*)$_2$}$_2$(ZnBr)$_5$(ZnCl)] (**3**).* [Cp*Fe(GaCp*)$_2$(GaBr$_2$)] (200 mg, 0.24 mmol) was dissolved in toluene (5 mL) and cooled to −30 °C. This solution was treated with 0.96 mL of a 2 M solution of $ZnMe_2$ (8 equiv, 1.93 mmol) in toluene and stirred for 1h at RT whereupon a deep red solution formed. After filtration of the mixture all volatile residues were removed in vacuo. Single crystals could be obtained by slow diffusion of hexane into a saturated solution of **3** in dichloromethane. Yield 152 mg (63%). ^{1}H NMR (250.1 MHz, CD_2Cl_2, 24 °C): δ = 2.07 (s, 60H, ZnCp*), 1.97 (s, 30H, FeCp*) ppm. ^{13}C NMR (62.9 MHz, CD_2Cl_2, 24 °C): δ = 112.4 (s, ZnC_5Me_5), 109.1 (s, FeC_5Me_5), 14.9 (s, FeC_5Me_5), 11.1 (s, ZnC_5Me_5) ppm. Elemental analytic data (dried sample in vacuo) calc. for Calc. for $Fe_2Zn_{10}Br_5Cl_1C_{60}H_{90}$: C, 35.8; H, 4.5; Zn, 32.5; found: C, 35.4; H, 4.5; Zn, 32.2, no gallium was detected.

Single Crystal X-ray Diffraction, Crystallographic and Structure Refinement Data. The X-ray intensity data were collected in the ω scan mode on an Oxford Diffraction Xcalibur2 diffractometer with a Sapphire2 CCD, using graphite-monochromatized Mo−Kα radiation (λ = 0.71073 Å). The data were processed with CrysAlisPro (Agilent Technologies). Absorption corrections were carried out semiempirically on the basis of multiple-scanned reflections with ABSPACK in CrysAlisPro. The crystal structures were solved (Table 6) by direct methods with SHELXS-97 and refined with SHELXL-97.[21] **1**·C_6H_5F was treated as a mixed crystal with the composition [Cp*Ru(ZnCp*)$_3$(ZnMe)(ZnX)]·C_6H_5F (X = Cl, Me), in which a chlorido ligand (Cl1) and a methyl group (C1′) statistically share the same site in the elementary cell of the single crystal. Although Zn−Cl and Zn−Me bonds are chemically not equivalent, Cl1 and C1′ were

dx.doi.org/10.1021/ic400741b | Inorg. Chem. 2013, 52, 7152−7160

refined with equal atomic coordinates and equal anisotropic displacement parameters as an approximation to stabilize the structural model. Refinement of the ratio of the occupancies by means of a free variable yielded a ratio of 0.326(3):0.674(3) between Cl1 and C1′. Note that different single crystals showed variation of the refined occupancies. The given data refer to the crystal which gave the best quality of the overall refinement. The fluorobenzene molecule in $\mathbf{1}\cdot C_6H_5F$ was found disordered about a crystallographic mirror plane, and was refined with rigid groups, partially equal anisotropic displacement parameters and restraints on geometry and displacement parameters. Severely disordered dichloromethane and hexane molecules in $\mathbf{3}\cdot CH_2Cl_2\cdot 0.5C_6H_{14}$ could not be modeled reasonably and were therefore removed from the diffraction data with Platon/SQUEEZE.[22] Hydrogen atoms were placed at geometrically calculated positions and refined with the appropriate riding model. Rotational disorder of methyl groups was found in $\mathbf{1}\cdot C_6H_5F$ and taken into account in the refinement. CCDC-929241 (**1**), CCDC-929241 (**2b**), and CCDC-929240 (**3**) contain the supplementary crystallographic data for this paper. These data can be obtained free of charge from the Cambridge Crystallographic Data Centre via www.ccdc.ac.uk/data_request/cif.

Computational Techniques and Details. We used the molecular structures of $[Cp^*Ru(ZnCp^*)_3(ZnMe)(ZnCl)]$, as well as $[Ru(ZnCp^*)_4(ZnMe)_6]$ and optimized at the BP86/def2-TZVPP[23] level with the Gaussian 03, Revision E.01[24] algorithm using energies, which were calculated with the Turbomole 6.3[25] program package. The resolution of the identity (RI) approximation[26] was applied using auxiliary basis functions.[27] Multipole accelerated RI-J (MARI-J)[28] was enabled. We obtained the optimized structures of the model compounds $[Cp^*Ru(ZnMe)_5]$, $[Cp^*Ru(ZnCl)_5]$, $[Ru(ZnCl)_{10}]$, and $[Ru(ZnMe)_{10}]$ in the same way. Frequencies and thermodynamic corrections were calculated with the aoforce[29] program out of the Turbomole package. The NBO[30] charges were obtained using the NBO 3.1 program implemented in Gaussian09, Revision A.02.[31] The AIM[32] analyses were carried out with the program package AIMAll[33] using a BP86/def2-TZVPP wave function created with Gaussian09. Energy-decomposition analyses (ETS-NOCV[34]) were carried out using the ADF(2012.02) program package at the BP86/TZ2P+ level of theory.[35] Not contracted Slater-type orbitals (STOs) were employed as basis functions in self-consistent field (SCF) calculations.[36] Triple-zeta-quality basis sets were used which were augmented by two sets of polarization functions, that is, p and d functions for the hydrogen atom and d and f functions for the other atoms. An auxiliary set of s, p, d, f and g STOs was used to fit the molecular densities and to represent the Coulomb and exchange potentials accurately in each SCF cycle.[38] Scalar relativistic effects were considered using the zero-order regular approximation (ZORA).[38] Within the EDA, bond formation between the interacting fragments is divided into three steps: In the first step, the fragments which are calculated with the frozen geometry of the entire molecule, are superimposed without electronic relaxation to yield the quasiclassical electrostatic attraction ΔE_{elstat}. In the second step, the product wave function becomes antisymmetrized and renormalized, which gives the repulsive term ΔE_{Pauli}, named the Pauli repulsion. The third step consists of the relaxation of the molecular orbitals to their final form to yield to stabilizing orbital interaction ΔE_{orb}. The sum of the three terms $\Delta E_{elstat}+ \Delta E_{Pauli}+ \Delta E_{orb}$ gives the total interaction energy ΔE_{int}.

■ ASSOCIATED CONTENT

Supporting Information

Further details are given in Tables S1−S5, and Figures S1−S6. This material is available free of charge via the Internet at http://pubs.acs.org.

■ AUTHOR INFORMATION

Corresponding Author

*E-mail: roland.fischer@ruhr-uni-bochum.de (R.A.F), frenking@chemie.uni-marburg.de (G.F.). Fax: (+49)234 321 4174 (R.A.F).

Notes

The authors declare no competing financial interest.

■ ACKNOWLEDGMENTS

This work was supported by German research Council (DFG, grant Fi 502/23-2). M.M. is grateful for a Ph.D. fellowship donated by the German Chemical Industry Fund (https://www.vci.de/fonds) and additional support by the Ruhr University Research School (http://www.research-school.rub.de).

■ REFERENCES

(1) (a) Cadenbach, T.; Bollermann, T.; Gemel, C.; Fernandez, I.; von Hopffgarten, M.; Frenking, G.; Fischer, R. A. *Angew. Chem., Int. Ed.* **2008**, *47*, 9150−9154. (b) Cadenbach, T.; Bollermann, T.; Gemel, C.; Tombul, M.; Fernandez, I.; van Hopffgarten, M.; Frenking, G.; Fischer, R. A. *J. Am. Chem. Soc.* **2009**, *131*, 16063−16077.

(2) (a) Bollermann, T.; Cadenbach, T.; Gemel, C.; Freitag, K.; Molon, M.; Gwildies, V.; Fischer, R. A. *Inorg. Chem.* **2011**, *50*, 5808−5814. (b) Jutzi, P.; Neumann, B.; Schebaum, L. O.; Stammler, A.; Stammler, H.-G. *Organometallics* **1999**, *18*, 4462−4464. (c) Gemel, C.; Steinke, T.; Cokoja, M.; Kempter, A.; Fischer, R. A. *Eur. J. Inorg. Chem.* **2004**, 4161−4176. (d) Gemel, C.; Steinke, T.; Weiss, D.; Cokoja, M.; Winter, M.; Fischer, R. A. *Organometallics* **2003**, *22*, 2705−2710.

(3) Molon, M.; Gemel, C.; von Hopffgarten, M.; Frenking, G.; Fischer, R. A. *Inorg. Chem.* **2011**, *50*, 12296−12302.

(4) Steinke, T.; Gemel, C.; Cokoja, M.; Winter, M.; Fischer, R. A. *Dalton Trans.* **2005**, 55−62.

(5) Cadenbach, T.; Gemel, C.; Fischer, R. A. *Angew. Chem., Int. Ed.* **2008**, *47*, 9146−9149.

(6) Molon, M.; Cadenbach, T.; Bollermann, T.; Gemel, C.; Fischer, R. A. *Chem. Commun.* **2010**, *46*, 5677−5679.

(7) Cokoja, M.; Gemel, C.; Steinke, T.; Schroeder, F.; Fischer, R. A. *Dalton Trans.* **2005**, 44−54.

(8) Allio, C.; Harbrecht, B. *Dalton Trans.* **2006**, 5352−5356.

(9) (a) del Rio, D.; Galindo, A.; Resa, I.; Carmona, E. *Angew. Chem., Int. Ed.* **2005**, *44*, 1244−1247. (b) Grirrane, A.; Resa, I.; Rodriguez, A.; Carmona, E.; Alvarez, E.; Gutierrez-Puebla, E.; Monge, A.; Galindo, A.; Del Rio, D.; Andersen, R. A. *J. Am. Chem. Soc.* **2007**, *129*, 693−703. (c) Resa, I.; Carmona, E.; Gutierrez-Puebla, E.; Monge, A. *Science (Washington, DC, U. S.)* **2004**, *306*, 411.

(10) (a) Wang, Y.; Quillian, B.; Wannere, C. S.; Wei, P.; Schleyer, P. v. R.; Robinson, G. H. *Organometallics* **2007**, *26*, 3054−3056. (b) Zhu, Z.; Brynda, M.; Wright, R. J.; Fischer, R. C.; Merrill, W. A.; Rivard, E.; Wolf, R.; Fettinger, J. C.; Olmstead, M. M.; Power, P. P. *J. Am. Chem. Soc.* **2007**, *129*, 10847−10857. (c) Al-Juaid, S. S.; Eaborn, C.; Habtemariam, A.; Hitchcock, P. B.; Smith, J. D.; Tavakkoli, K.; Webb, A. D. *J. Organomet. Chem.* **1993**, *462*, 45−55.

(11) Cadenbach, T.; Gemel, C.; Bollermann, T.; Fischer, R. A. *Inorg. Chem.* **2009**, *48*, 5021−5026.

(12) Cadenbach, T.; Gemel, C.; Schmid, R.; Halbherr, M.; Yusenko, K.; Cokoja, M.; Fischer, R. A. *Angew. Chem., Int. Ed.* **2009**, *48*, 3872−3876.

(13) Cadenbach, T. *Zwischen Koordinationsverbindungen und Clustern: Prinzipien und Konzepte zur Synthese hochkoordinierter, metallreicher Moleküle*. Dissertation, Ruhr-Universität Bochum, Bochum, Germany, 2009.

(14) Buchin, B.; Gemel, C.; Kempter, A.; Cadenbach, T.; Fischer, R. A. *Inorg. Chim. Acta* **2006**, *359*, 4833−4839.

(15) (a) Sousa-Pedrares, A.; Duran, M. L.; Romero, J.; Garcia-Vazquez, J. A.; Monteagudo, J. C.; Sousa, A.; Dilworth, J. R. *Inorg. Chim. Acta* **2006**, *359*, 863−876. (b) Wright, J. A.; Danopoulos, A. A.;

Motherwell, W. B.; Carroll, R. J.; Ellwood, S.; Saßmannshausen, J. *Eur. J. Inorg. Chem.* **2006**, *2006*, 4857−4865.
(16) Bollermann, T.; Schwedler, I.; Molon, M.; Freitag, K.; Gemel, C.; Seidel, R. W.; Fischer, R. A. *Dalton Trans.* **2011**, 12570−12577.
(17) (a) Zabrodsky, H.; Peleg, S.; Avnir, D. *J. Am. Chem. Soc.* **1992**, *114*, 7843−51. (b) Zabrodsky, H.; Peleg, S.; Avnir, D. *J. Am. Chem. Soc.* **1993**, *115*, 8278−89. (c) Pinsky, M.; Avnir, D. *Inorg. Chem.* **1998**, *37*, 5575−5582.
(18) Cirera, J.; Ruiz, E.; Alvarez, S. *Organometallics* **2005**, *24*, 1556−1562.
(19) Ruiz-Martínez, A.; Alvarez, S. *Chem.—Eur. J.* **2009**, *15*, 7470−7480.
(20) Häussermann, U.; Viklund, P.; Svensson, C.; Eriksson, S.; Berastegui, P.; Lidin, S. *Angew. Chem., Int. Ed.* **1999**, 488−492.
(21) (a) Sheldrick, G. M., *SHELXL-97, Program for refinement of crystal structures*; University of Göttingen: Göttingen, Germany, 1997; (b) Sheldrick, G. M. *Acta Crystallogr., Sect. A Found. Crystallogr.* **2008**, *A64*, 112−122.
(22) (a) Sluis, P. v. d.; Spek, A. L. *Acta Crystallogr.* **1990**, *46*, 194−201. (b) Spek, A. L. *J. Appl. Crystallogr.* **2003**, *36*, 7−13.
(23) (a) Becke, A. D. *Phys. Rev. A* **1988**, *38*, 3098−3100. (b) Perdew, J. *Phys. Rev. B* **1986**, *33*, 8822−8824. (c) Weigend, F.; Ahlrichs, R. *Phys. Chem. Chem. Phys.* **2005**, *7*, 3297−305.
(24) Frisch, M. J.; Trucks, G. W.; Schlegel, H. B.; Scuseria, G. E.; Robb, M. A.; Cheeseman, R. J.; Montgomery, Jr., J. A.; Vreven, T.; Kudin, K. N.; Burant, J. C.; Millam, J. M.; Iyengar, S. S.; Tomasi, J.; Barone, V.; Mennucci, B.; Cossi, M.; Scalmani, G.; Rega, N.; Petersson, G. A.; Nakatsuji, H.; Hada, M.; Ehara, M.; Toyota, K.; Fukuda, R.; Hasegawa, J.; Ishida, M.; Nakajima, T.; Honda, Y.; Kitao, O.; Nakai, H.; Klene, M.; Li, X.; Knox, J. E.; Hratchian, H. P.; Cross, J. B.; Bakken, V.; Adamo, C.; Jaramillo, J.; Gomperts, R.; Stratmann, R. E.; Yazyev, O.; Austin, A. J.; Cammi, R.; Pomelli, C.; Ochterski, J. W.; Ayala, P. Y.; Morokuma, K.; Voth, G. A.; Salvador, P.; Dannenberg, J. J.; Zakrzewski, V. G.; Dapprich, S.; Daniels, A. D.; Strain, M. C.; Farkas, O.; Malick, D. K.; Rabuck, A. D.; Raghavachari, K.; Foresman, J. B.; Ortiz, J. V.; Cui, Q.; Baboul, A. G.; Clifford, S.; Cioslowski, J.; Stefanov, B. B.; Liu, G.; Liashenko, A.; Piskorz, P.; Komaromi, I.; Martin, R. L.; Fox, D. J.; Keith, T.; Al-Laham, M. A.; Peng, C. Y.; Nanayakkara, A.; Challacombe, M.; Gill, P. M. W.; Johnson, B.; Chen, W.; Wong, M. W.; Gonzalez, C.; Pople, J. A. *Gaussian 03*; Gaussian Inc.: Wallingford, CT, 2004.
(25) van der Sluis, P.; Spek, A. L. *Acta Crystallogr. Sect. A* **1990**, *46*, 194−201.
(26) Ahlrichs, R. *Phys. Chem. Chem. Phys.* **2004**, *6*, 5119−5124.
(27) (a) Eichkorn, K.; Treutler, O.; Häser, M.; Ahlrichs, R. *Chem. Phys. Lett.* **1995**, *242*, 652−660. (b) Eichkorn, K.; Weigend, F.; Treutler, O.; Ahlrichs, R. *Theor. Chem. Acc.* **1997**, *97*, 119−124. (c) Weigend, F. *Phys. Chem. Chem. Phys.* **2006**, *8*, 1057−1065.
(28) Sierka, M.; Hogekamp, A.; Ahlrichs, R. *J. Chem. Phys.* **2003**, *118*, 9136−9144.
(29) (a) Deglmann, P.; May, K.; Furche, F.; Ahlrichs, R. *Chem. Phys. Lett.* **2004**, *384*, 103. (b) Deglmann, P.; Furche, F.; Ahlrichs, R. *Chem. Phys. Lett.* **2001**, *362*, 511. (c) Deglmann, P.; Furche, F. *J. Chem. Phys.* **2002**, *117*, 9535−9538.
(30) (a) Reed, A. E.; Weinstock, R. B.; Weinhold, F. *J. Chem. Phys.* **1985**, *83*, 735. (b) Reed, A. E.; Curtiss, L. A.; Weinhold, F. *Chem. Rev.* **1988**, *88*, 899−926.
(31) Frisch, M. J.; Trucks, G. W.; Schlegel, H. B.; Scuseria, G. E.; Robb, M. A.; Cheeseman, J. R.; Scalmani, G.; Barone, V.; Mennucci, B.; Petersson, G. A.; Nakatsuji, H.; Caricato, M.; Li, X.; Hratchian, H. P.; Izmaylov, A. F.; Bloino, J.; Zheng, G.; Sonnenberg, J. L.; Hada, M.; Ehara, M.; Toyota, K.; Fukuda, R.; Hasegawa, J.; Ishida, M.; Nakajima, T.; Honda, Y.; Kitao, O.; Nakai, H.; Vreven, T.; Montgomery, J. A., Jr.; Peralta, J. E.; Ogliaro, F.; Bearpark, M.; Heyd, J. J.; Brothers, E.; Kudin, K, N.; Staroverov, V. N.; Kobayashi, R.; Normand, J.; Raghavachari, K.; Rendell, A.; Burant, J. C.; Iyengar, S. S.; Tomasi, J.; Cossi, M.; Rega, N.; Millam, N. J.; Klene, M.; Knox, J. E.; Cross, J. B.; Bakken, V.; Adamo, C.; Jaramillo, J.; Gomperts, R.; Stratmann, R. E.; Yazyev, O.; Austin, A. J.; Cammi, R.; Pomelli, C.; Ochterski, J. W.; Martin, R. L.; Morokuma, K.; Zakrzewski, V. G.; Voth, G. A.; Salvador, P.; Dannenberg, J. J.; Dapprich, S.; Daniels, A. D.; Farkas, O.; Foresman, J. B.; Ortiz, J. V.; Cioslowski, J.; Fox, D. J. *Gaussian 09*, Revision A; Gaussian, Inc.: Wallingford, CT, 2009.
(32) Bader, R. F. W. *Atoms in Molecules: A Quantum Theory*; Oxford University Press: Oxford, U.K., 1990.
(33) *AIMAll*: http://aim.tkgristmill.com
(34) (a) Nalewajski, R. F.; Mrozek, J.; Michalak, A. *Int. J. Quantum Chem.* **1997**, *61*, 589. (b) Michalak, A.; De Kock, R. L.; Ziegler, T. *J. Phys. Chem. A* **2008**, *112*, 7256.
(35) *ADF2012.01*; SCM, Theoretical Chemistry, Vrije Universiteit: Amsterdam, The Netherlands; http://www.scm.com.
(36) Snijders, J. G.; Vernooijs, P.; Baerends, E. J. *At. Data Nucl. Data Tables* **1981**, *26*, 483−509.
(37) Krijn, J.; Baerends, E. J. *Internal Report: Fit Functions in the HFSMethod*; Vrije Universiteit: Amsterdam, The Netherlands, 1984.
(38) (a) Chang, C.; Pelissier, M.; Durand, P. *Phys. Scr.* **1986**, *34*, 394−404. (b) Heully, J.-L.; Lindgren, I.; Lindroth, E.; Lundqvist, S.; Martensson-Pendrill, A.-M. *J. Phys. B* **1986**, *19*, 2799. (c) Snijders, J. *Chem. Phys. Lett.* **1996**, *252*, 51−61. (d) Lenthe, E. V.; Baerends, E. J.; Snijders, J. G. *J. Chem. Phys.* **1993**, *99*, 4597. (e) van Lenthe, E.; van Leeuwen, R.; Baerends, E. J.; Snijders, J. G. *Int. J. Quantum Chem.* **1996**, *57*, 281−293.
(39) One referee pointed out that the Zn-Zn distance is shorter than the sum of the van der Waals radii and therefore, some bonding interactions should be expected. The reviewer suggested that we reoptimize the geometry of $[Cp^*Ru(ZnMe)_5]$ with inclusion of dispersion forces. We followed the suggestion of the referee and optimized the geometry at BP86-D3/TZVPP using Grimme's correction D3 for dispersion interaction.[40] The geometry changed only marginally and the AIM analysis of the BP86-D3/TZVPP optimized structure did not show a Zn-Zn path. The rather weak Zn-Zn bonding, which yield Wiberg bond orders of only 0.04−0.06, are not sufficient to give a bond path. A similar situation was reported by us in reference 1 where we showed that the complex $[Mo(ZnMe)_{12}]$ has 12 bond paths for the Mo-Zn bonding but no Zn-Zn bond path, although the orbital analysis indicates weak attractive interactions. It has been shown in numerous previous papers[41] that a bond path is neither a sufficient nor a necessary criterion for a chemical bond. It is the combination of the shape of the Laplacian distribution and the absence of the bond path which let us suggest that there are no genuine Zn-Zn chemical bonds in $[Cp^*Ru(ZnMe)_5]$.
(40) Grimme, S.; Antony, J.; Ehrlich, S.; Krieg, H. *J. Chem. Phys.* **2010**, *132*, 154104.
(41) (a) Haaland, A.; Shorokhov, D. J.; Tverdova, N. V. *Chem.—Eur. J.* **2004**, *10*, 4416. (b) Bader, R. F. W.; Fang, D.-C. *J. Chem. Theory Comput.* **2005**, *1*, 403. (c) Poater, J.; Solà, M.; Bickelhaupt, F. M. *Chem.—Eur. J.* **2006**, *12*, 2902. (d) Krapp, A.; Frenking, G. *Chem.—Eur. J.* **2007**, *13*, 8256. (e) Strenalyuk, T.; Haaland, A. *Chem.—Eur. J.* **2008**, *14*, 10223. (f) von Hopffgarten, M.; Frenking, G. *Chem.—Eur. J.* **2008**, *14*, 10227. (g) Mousavi, M.; Frenking, G. *Organometallics* **2013**, *32*, 1743. (h) Mousavi, M.; Frenking, G. *J. Organomet. Chem.*, 10.1016/j.jorganchem.2013.03.047.